



Nonpyrogenic charring of Late Pleistocene large mammal remains in northeastern Russia

IRINA V. KIRILLOVA , OLGA K. BORISOVA, OLGA F. CHERNOVA, GARY HAYNES , NINA V. NARINA, ANDREY V. PANIN, OKSANA G. ZANINA, ELYA P. ZAZOVSKAYA, ANDREY Y. ZHURAVLEV AND VIKTOR N. ZVYAGIN

BOREAS



Kirillova, I. V., Borisova, O. K., Chernova, O. F., Haynes, G., Narina, N. V., Panin, A. V., Zanina, O. G., Zazovskaya, E. P., Zhuravlev, A. Y. & Zvyagin, V. N. 2022 (April): Nonpyrogenic charring of Late Pleistocene large mammal remains in northeastern Russia. *Boreas*, Vol. 51, pp. 481–495. <https://doi.org/10.1111/bor.12569>. ISSN 0300-9483.

Mammal remains preserved in the permafrost zone often bear traces of postmortem transformations, reflecting aspects of the palaeoenvironment and the processes that took place during the accumulation of host sediments. Multidisciplinary studies including radiocarbon dating, infrared spectroscopy, and microfossil analyses and grain size of infilling sediments from remains allow recognition of their stratigraphical and palaeogeographical origins and facilitate reconstructions of taphonomic pathways and the pre-burial environments. Here, as exemplified by skulls of woolly rhinoceros, cave lion, and ancient bison, some distinct features of postmortem changes such as nonpyrogenic charring and vivianite encrustation indicate that the remains have undergone a complex range of burial processes in aerobic and anaerobic conditions in the Pleistocene landscapes of Arctic northeastern Russia. We hypothesize that these processes were mainly confined to the warmer intervals in the Late Pleistocene.

Irina V. Kirillova (ikirillova@yandex.ru), Olga K. Borisova, Andrey V. Panin and Elya P. Zazovskaya, Institute of Geography, Russian Academy of Sciences, Staromonetny Lane 29, Moscow 119017, Russia; Olga F. Chernova, A.N. Severtsov Institute of Ecology and Evolution, Russian Academy of Sciences, Leninskiy Prt. 33, Moscow 119071, Russia; Gary Haynes, Department of Anthropology, University of Nevada-Reno, 1755 Allen Str., Reno, Nevada 89509, USA; Nina V. Narina and Viktor N. Zvyagin, Russian Center of Forensic Medical Expertise, Ministry of Healthcare, Polikarpov Str. 12/13, Moscow 125284, Russia; Oksana G. Zanina, Institute of Physicochemical and Biological Problems in Soil Science, Institutskaya Str. 2, Pushchino, Moscow region 142290, Russia; Andrey Y. Zhuravlev, Lomonosov Moscow State University, Leninskie Gory 1(12), Moscow 119234, Russia; received 17th August 2021, accepted 9th October 2021.

The remains of mammoth fauna representatives include famous well-preserved mummies and carcasses in the extreme northeast of Russia. Most often they have been surface finds, and much less often were discovered in geological sections. The task of researchers is to determine the stratigraphical level from which a certain specimen originated and to reconstruct the burial pathways and palaeohabitat. Indeed, a study of the preservation of such finds makes it possible not only to associate the remains with a geological section, but also to distinguish faunal assemblages. For instance, such a study of Pleistocene remains from the Lower Volga River basin of southern European Russia allowed them to be subdivided into several assemblages by the degree of postmortem transformation (Gromov 1948). Similarly, scattered bones from the Kor & Bot collection, originating from Oosterschelde estuary sediments in the Netherlands, were divided after a recent revision into several faunal groups of greatly diverging age defined by species composition, diversity, and taphonomic features (Scager *et al.* 2017).

It is noteworthy that the processes that mix variously preserved bones from different individuals and species begin as early as they do for carcasses lying on ground surfaces because carnivores and scavengers quickly disarticulate them and disperse bones (Haynes 1981, 1988).

In the northern permafrost zone, animal remains change little from the state in which they were buried, due to low temperatures, common anaerobic conditions and acidic milieu that drastically slow down or block microorganism activity. They are mostly restricted to ice-rich fine-grained perennially frozen grounds or yedoma, which are widespread in northeastern Russia. The remains are preserved until exposed by the activity of natural agents or by humans. In perennially frozen sediments the process of fossilization – i.e. loss of the organic part of bone and replacement of its biomineral components – usually does not occur or is greatly slowed (Smirnov *et al.* 2009). This is demonstrated by finds of well-preserved animal mummies and carcasses (Guthrie 1990; Boeskov *et al.* 2011; van Geel *et al.* 2011; Spasskaya *et al.* 2012; Kirillova *et al.* 2015). Additionally, carbon-rich Pleistocene bones can be reliably ¹⁴C dated and studied with other methods such as isotope analysis (e.g. Bronk Ramsey *et al.* 2004). By defining common features of different finds, bone beds can be distinguished and the search for more discoveries can be expanded. A study of bone preservation and taphonomic features of fossil sites can facilitate reconstruction of burial palaeoenvironments.

It is often difficult to determine the conditions that affected the preservation of bone residues: for example,

blackening can be caused by removal of organic components due to wildfires or through the destruction of mineral components by chemical compounds (acid, alkali) formed by decomposing organic matter in host sediments; blackening also may result from enrichment in iron, manganese, and rare earth elements. Well-known examples are the human ‘bog bodies’, which were turned dark brown by the tanning effect of either *Sphagnum* polymers or due to electrostatic interactions between body genuine amino groups and sugars (Giles 2020). In the modern cold northern regions, mammalian remains often acquire a dark brown or black tint due to nonpyrogenic processes in the seasonally active ground (Pletyanova 2016). The bones look charred as if burned, but they are covered or impregnated with metal salts or they have been blackened by microorganismic activities.

The purposes of the study reported here are (i) to determine the causes of some transformations of Late Pleistocene mammalian remains from permafrost areas of northeastern Russia, and (ii) to use a high-resolution multidisciplinary approach to reconstruct conditions causing these transformations, as well as the pre-burial and burial environments.

Geological setting, material and methods

In the Arctic northeast of Russia, including the vast coastal lowlands (Yano-Indigiro-Kolyma) in the north of Yakutia, ice-rich permafrost or *edoma* and taberal deposits are widespread. These are mainly Late Pleistocene in age, and contain accumulations of mammalian remains (Sher 1974; Vereshchagin 1979; Lazarev & Tomskaya 1987). *Edoma* includes ice wedges and consists of fine-grained loess-like silts with interlayers of peat and palaeosoils of varying thickness (e.g. Tomirdiaro & Chernen'ky 1987; Sher *et al.* 2005; Murton *et al.* 2015, and references therein). Due to the regular seasonal thawing of permafrost, the remains of ancient mammals are transported and accumulated in river valleys, lakes and coasts. Despite the lack of precise stratigraphical origins, this material provides a valuable database for taphonomic, palaeoecological, and other scientific reconstructions.

The present study selected blackened Pleistocene mammalian remains that were collected by local residents from northeastern Russia (Fig. 1) and are housed in the National Alliance of Shidlovskiy ‘Ice Age’ collection, Moscow. These are: (i) skulls of the cave lion (*Panthera spelaea*) F-4299, ancient bison (*Bison priscus*) F-4236, and woolly rhinoceros (*Coelodonta antiquitatis*) F-61 from the middle–lower reaches of the Indigirka River, upstream of Chokurdakh township (near latitude 68°35'N, longitude 147°06'E); (ii) skull, mandible, nasal, and frontal horns of a single individual of woolly rhinoceros, F-506–F-509 from the channel of the Malaya Kuropatoch'ya River, about 2 km above the mouth

(near 71°01'N, 155°35'E); (iii) nasal horn of woolly rhinoceros F-1990 from the vicinity of Chersky township, Lower Kolyma River (near 68°44'N, 161°21'E).

From the cerebral cavity of the skulls of F-4299, F-506 and F-61, sediment infilling samples were taken to analyse the granulometric composition and perform palaeobotanical studies.

A human skull had been exhumed on the Island Bely, near the Kara Sea coast (73°20'N, 70°45'E) during fieldwork under the regional project ‘Kara Expeditions’ patronaged by the government of the Yamal-Nenets Autonomous District, Russia, in 2015 for forensic purposes. It was re-buried in its original grave after study (Pletyanova 2016).

Grain-size analysis

Grain-size analysis of infilling sediments from brain cases of skulls F-4299, F-506, and F-61 was performed by laser diffractometry on a Malvern Mastersizer 3000 granulometer in the Institute of Geography, Russian Academy of Sciences (RAS), Moscow. Only silicate minerals of the sediment were analysed as they are less prone to diagenesis. Organic matter and carbonates were removed during the preliminary preparation. Preparation of samples included sequential treatment with a 10% solution of hydrochloric acid (1 h) and a 30% solution of hydrogen peroxide heated in a water bath to 90 °C (over 3 h, before bleaching the material). After treatment with reagents, the material was transferred with a pipette to the liquid cell of the dispersion unit of the Hydro EV analyser. In the cell, the material was exposed for 100 s to ultrasound with a capacity of 70% and was intensively mixed with a special turntable at a speed of 2400 rpm. Particle sizes were calculated based on the Mi model with standard values (Ozer *et al.* 2010) for the refractive index and absorption ($n = 1.45$; $k = 0.1$).

Pollen analysis

For the pollen analysis, two samples of the infilling sediment were extracted from the F-506 and F-61 woolly rhinoceros skull cavities. Pollen and spores were separated from the sediment following Grichuk's (1940) method of using a heavy liquid (CdI solution) with a density of 2.2 g cm⁻³. These were examined under a light microscope with a magnification of 400×. In samples F-506 and F-61, all terrestrial pollen grains and spores from two pollen slides were counted to calculate percentages of the most common taxa. Ten additional pollen slides from each sample were scanned to detect rare palynomorphs.

Biogenic fraction analysis

Other microfossils (phytoliths, diatoms, sponge spicules) from the infilling sediment in the F-506 woolly rhinoceros skull were isolated in accordance with the

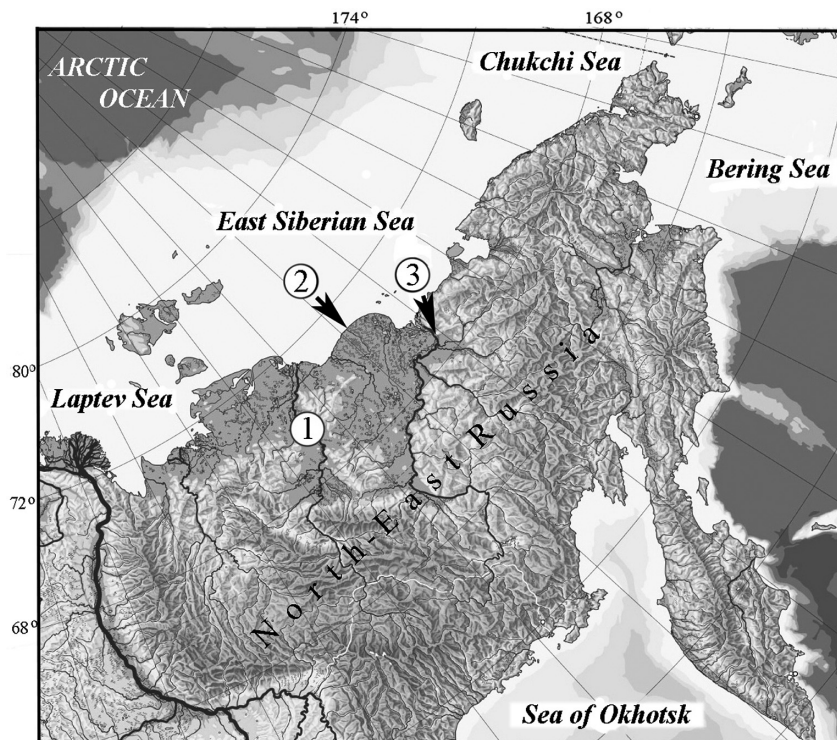


Fig. 1. Northeastern Siberia showing the localities of fossil finds. 1 = Middle–lower course of the Indigirka River (skulls of woolly rhinoceros F-61, ancient bison F-4236 and cave lion F-4299). 2 = Lower reaches of the Malaya Kuropatoch'ya River (skull, mandible, and both horns from a single woolly rhinoceros individual F-506–F-509). 3 = Lower reaches of the Kolyma River (horn of woolly rhinoceros F-1990).

procedure described in Kirillova *et al.* (2020). The resulting material in glycerine was examined under a Carl Zeiss Axiostar Plus microscope, 100–400 \times , at pH 2. Measurement of microfossils from the dried sample was carried out under a Vega 3 Tescan scanning electron microscope (SEM) in high and variable vacuum mode accompanied by BSE and SE analysers in the Institute of Physicochemical and Biological Problems of Soil Science, Pushchino.

Radiocarbon dating

Preparation for radiocarbon bone and tooth dating was carried out in the Laboratory of Radiocarbon Dating and Electron Microscopy of the Institute of Geography, RAS (laboratory index IGANAMS), using accelerator mass spectrometry (AMS). Collagen isolation for AMS dating complied with the standard protocol (Brown *et al.* 1988), supplemented by ultrafiltration (Bronk Ramsey *et al.* 2004). Graphitization of samples was performed using the AGE3 system combined with a vario ISOTOPE select element analyzer (Elementar, UK; Nemeč *et al.* 2010). The resulting graphites were compressed into the NEC target with a pneumatic press (PSP, Ionplus). The measurement of radiocarbon age was carried out at the Center for Applied Isotopic Research at the University of Geor-

gia, USA (CAIS). The $^{14}\text{C}/^{13}\text{C}$ ratio in graphite was measured on a 0.5 MeV tandem system accelerator-mass spectrometer 1.5SDH-1 Pelletron AMS. All measurements were made against the OXII standard; the radiocarbon age was calculated using the Libby half-life of 5568 years. Dates were adjusted for natural isotopic fractionation. Calibration was performed in OxCAL using the IntCal13 calibration curve (Reimer *et al.* 2013).

Infrared spectrophotometry

For the study, samples with the most pronounced blackening were selected, specifically the mandible F-509 and the nasal horn F-507 of a single woolly rhinoceros individual. The study was conducted on a Nicolet iS 10 FTIR spectrometer in the Russian Centre of Forensic Medical Expertise in order to obtain information on the composition of organic and inorganic components of tissues (bone, horn). The samples (fragments) were the following: Sample 1 – mandible, 24 \times 20 mm, strongly charred side; Sample 2 – mandible, 24 \times 20 mm, less charred side; Sample 3 – blackened horn, 11 \times 46 mm; Sample 4 – mandible, 24 \times 20 mm, tip, minimal external changes.

A control sample (Control 1) was represented by an unmodified bone fragment from the skeleton of a

25–30 years old human male, postmortem interval 3 years. The objects were thoroughly rubbed in an agate mortar for 15 min, and a 2.5 mg sample weight was mixed with 250 mg of dried KBr and re-rubbed for 10 min in an agate mortar. From the resulting mixture, a pellet was made using a Graseby Specac manual hydraulic press. The background object was a similarly manufactured pellet of carefully dried and grated powder KBr. The spectrum of the pellet was fixed in the frequency range 450–4000 cm^{-1} . Decoding of infrared spectra of bone tissue was carried out according to the Shafrenskiy method (Mikhailov *et al.* 1987).

Results

Taphonomic features and radiocarbon ages of fossil skulls

The skull, mandible, and both horns (F-506–F-509) of a single woolly rhinoceros individual (Fig. 2) were discovered in association during underwater studies of the Malaya Kuropatoch'ya River in a deep hollow of the watercourse. In the wet state, the horns were plastic and easily deformed, but they hardened when dried. The colour of all the specimens in the wet state was black; in the dry state, they turned to be blackish-brown. The intensity of the black tint of the skull is highest on the surface, and the colour is lighter deeper in the tissue. The nasal horn has lost its lateral filaments, is flattened, and

black throughout; the surface is uneven. The frontal horn is better preserved, at the base it is coloured unevenly, which emphasizes its structure: the outermost part is the darkest; the middle is lighter; the innermost part, the densest in the horn (Chernova & Kirillova 2010), stands out with a relatively darker colour (Fig. 2B).

Nasal horn F-1990 has visually similar preservation (Fig. 2C), with the difference that some places on its surface preserved undamaged areas (thin, up to 1–2 mm crust) of grey colour; under which, however, the bone tissue is also blackened.

Less pronounced blackening is also seen on the cave lion skull F-4299 in the front part, in the area of the nasal bones, and on the horn cover of the ancient bison F-4236 horn; the latter sample is covered with a thin blue encrustation in a dry state (Fig. 3). The results of ^{14}C dating of specimens are given in Table 1.

Grain-size composition of infilling deposits

Analysis of the infilling sediments from the skulls of F-4299, F-506, and F-61 by laser granulometry revealed very close single-mode distributions of particle size ranges with a maximum at 25–40 μm and median diameter of 16 to 20 μm (Fig. 4). The peak falls on the fraction of coarse silt (10–50 μm), which represented about half of the sediment (50–54%), and silt in general (5–50 μm) accounts for up to 2/3 of the sediment: 65, 67

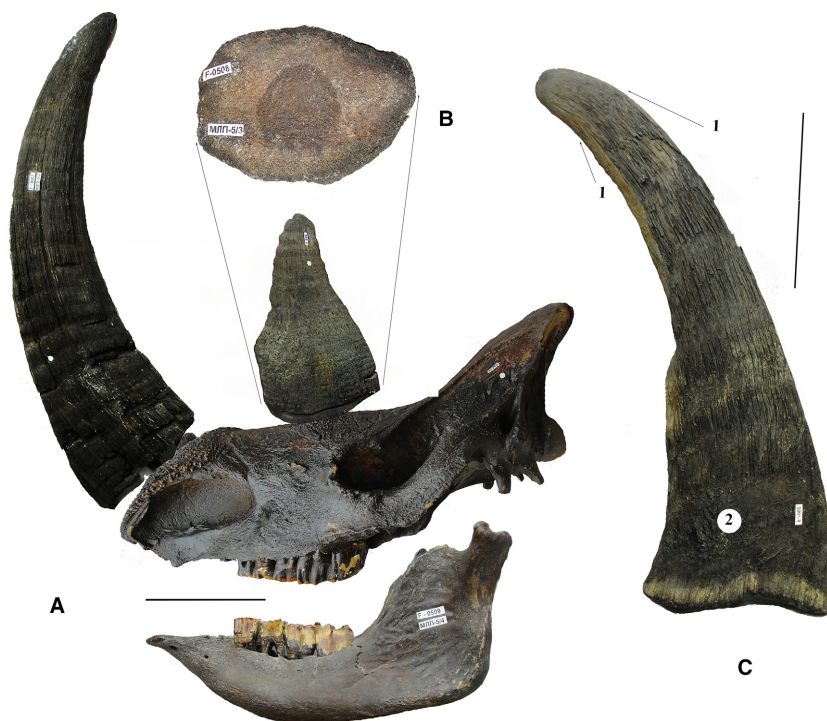


Fig. 2. Charred remains of a single woolly rhinoceros individual. A. Associated F-506 skull, F-507 nasal horn, F-508 frontal horn and F-509 mandible of one individual, side view. B. Frontal horn as above, from the base. C. Nasal horn F-1990: 1 = outer (grey) part; 2 = inner (dark) part. National Alliance of Shidlovskiy 'Ice Age', Moscow. Scale bar: 20 cm.

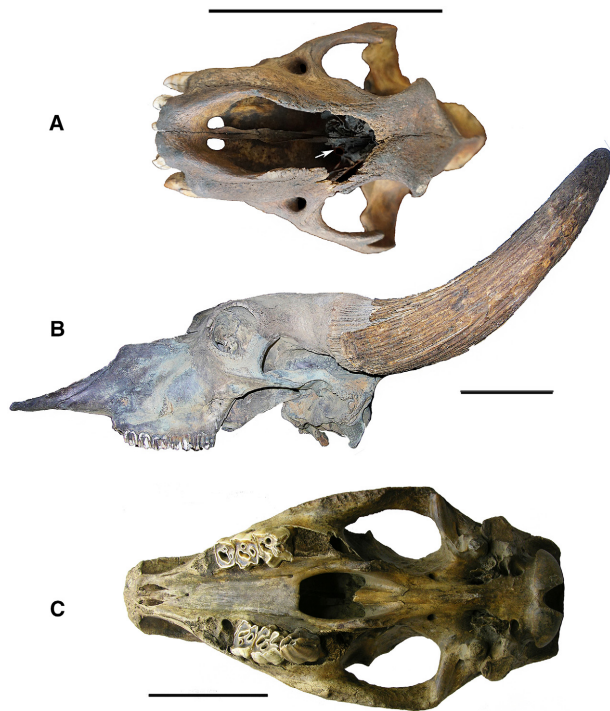


Fig. 3. Charred skulls. A. Cave lion F-4299 (view from above). B. Ancient bison with charred horn core F-4236 (side view), whitish cover of vivianite on the skull is also visible. C. Woolly rhinoceros F-61 (bottom view). National Alliance of Shidlovskiy 'Ice Age', Moscow. Scale bar: 20 cm.

and 66%, respectively. Sand (50–1000 μm) accounts for 13, 14 and 14%, with fine-grained sand (50–100 μm) dominating. The maximum particle size is 400–500 μm (medium-grained sand).

Biogenic fraction analysis

Diatoms. – Frustules and separate valves of diatoms of at least 10 species belonging to the Pleistocene and extant freshwater unicellulars were found in specimen F-506. Some frustules are quite large, about 120 μm in diameter. The valves are thin-walled and fragile, strongly perforated; their integrity implies the absence of long-range transportation and redeposition. *Navicula radiosa* Kützing, *Stauroneis* sp., *Pinnularia* species including *P. borealis* Ehrenberg, *Cocconeis placentula* Ehrenberg, *Cymbella* sp., *Didymosphenia geminata* (Lyngbye) M. Schmidt, *Gomphonema* sp., *Ulnaria*

sp., and palustrine species of the genus *Eunotia* were determined. The species are illustrated by SEM images (Fig. S1).

Sponges. – Multiple fragmented sponges are represented including single megascleres of oxea type. Oxea megascleres probably belong to representatives of the family Spongillidae. According to the geographical distribution of genera of this family, the spicules derived from either *Spongilla* or *Ephydatia*, which are the only genera occurring in Arctic Asia (Manconi & Pronzato 2002).

Phytoliths. – A large number of various phytoliths were discovered in specimen F-506 (Fig. S2). Lobed trapezoid symmetrical and asymmetrical particles dominated. Trychomes with a wide base are subdominants; there are elongated cylindrical forms of 10–50 μm in length, with a wavy edge, which is typical for graminoids. Elongated smooth cylindrical forms are produced in the leaves and culms of both graminoid and dicotyledonous herbs.

Pollen. – In the infilling sediment of the skull F-506, arboreal (tree and shrub) pollen (AP) content reaches 30% of the total terrestrial pollen and spore sum (Σ). Pollen of trees is represented mainly by *Betula* sect. *Albae* (about 10% of Σ) (Table S1). A small amount of pine pollen from *Pinus sylvestris*, *P. sibirica* and *P. pumila*, and rare pollen grains of *Larix* were also recorded (Table S1). *Duschekia fruticosa*, *Betula* sect. *Fruticosae*, *B.* sect. *Nanae* and willow species prevail among the shrubs. The pollen of non-arboreal plants (grass, herbs and dwarf shrubs) – NAP – constitutes 63% of Σ . NAP is dominated by the Poaceae (18% of Σ) and *Artemisia* (12% of Σ), with a noticeable share of Cyperaceae, Ericales, Caryophyllaceae and Saxifragaceae. Small fragments of sedge roots and rhizomes were also found. The NAP in sample F-506 is extremely diverse: there are over 15 families (e.g. Asteraceae, Cichoriaceae, Ranunculaceae, Rosaceae, Polygonaceae). As well, pollen was identified from typical meadow plants of the tundra and forest-tundra zones, e.g. *Polemonium*, *Pedicularis* and *Valeriana*. Spores make up 7% of Σ ; among them *Sphagnum* and *Riccia* predominate.

In the infilling sediment from the skull F-61, AP makes up 45% of Σ , NAP: 48%, and spores: 6% of the sum

Table 1. Radiocarbon dating results.

Specimen	Lab no. IGAN _{AMS}	Tissue	C/N (%)	¹⁴ C age (a BP; 1 σ)	Mean age (cal. a BP; 1 σ) (source)
F-4299, cave lion	6916	Bone	3.24	25 030 \pm 70	29 070 \pm 140 (herein)
F-4236, bison	6921	Tooth root	3.38	36 805 \pm 170	41 430 \pm 180 (herein)
F-507, woolly rhinoceros	6917	Tooth root	3.25	39 500 \pm 180	43 190 \pm 190 (Puzachenko <i>et al.</i> 2021)

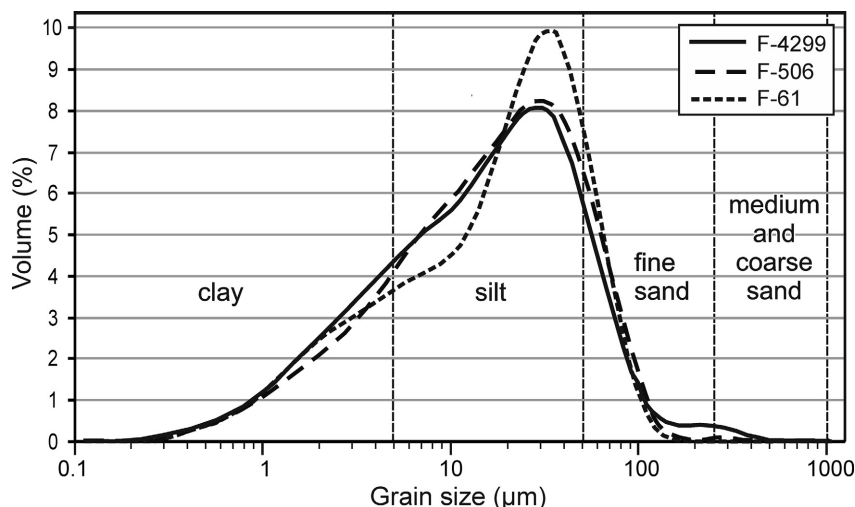


Fig. 4. Grain-size composition of infilling sediments (logarithmic scale) from the skulls of cave lion F-4299 and woolly rhinoceroses F-506 and F-61.

(Table S1). The content of *Larix* pollen reaches 5% of Σ , which taking into account its low resistance to decomposition indicates a significant role of larch in the local vegetation. Fragments of the epidermis of larch needles with stomata found in sample F-61 clearly indicate the presence of *Larix*. Among the AP, pollen of tree and shrub birches dominates (about 22% of Σ). *Salix* pollen is about 8%, shrub alder pollen is 6% of Σ . Rare pollen of *Pinus pumila*, *P. sylvestris* and *Picea* were also found. The NAP is represented mainly by Cyperaceae (21%) and Poaceae (16% of Σ). The pollen contents of Asteraceae, Cichoriaceae, Polygonaceae, Caryophyllaceae and Onagraceae do not exceed 2% of Σ ; the remainder of herbaceous plants are represented by rare pollen grains. The sample also contained a few spores of *Sphagnum*, Hepaticae, *Equisetum* and *Selaginella rupestris* as well as rare pollen grains of aquatic and sub-aquatic plants and coenobia of *Pediastrum* and *Botryococcus* green algae (Table S1).

Infrared spectral study

In the IR absorption spectrum of the control sample (fresh human bone; Fig. 5), the most commonly observed bands were intense absorption bands associated with splitting in the PO_4^{3-} region at $500\text{--}650\text{ cm}^{-1}$ (deformation vibrations), $900\text{--}1150\text{ cm}^{-1}$ (valence vibrations), anion absorption bands CO_3^{2-} at 880, 1430 and 1460 cm^{-1} , absorption bands related to vibrations in the protein region (amide III 1240 cm^{-1} , amide II $1540\pm 10\text{ cm}^{-1}$, amide I $1660\pm 20\text{ cm}^{-1}$) including methyl CH_2 and CH_3 groups ($2850\pm 30\text{ cm}^{-1}$, $2925\text{--}2970\text{ cm}^{-1}$), and a lipid absorption band at $1740\pm 15\text{ cm}^{-1}$. Absorption bands at 570, 610, 1050, 1120, 1430 and 1460 cm^{-1} characterize the orthophosphate crystal lattice of the bone $[\text{Ca}_{10}(\text{PO}_4)_6(\text{OH})_2]$.

Thus, the IR absorption spectrum of the control sample contains almost all the peaks being analysed except for lipids (in region at 1740 cm^{-1}). There are peaks of the specific shape and proportion being indicative of amide intensity I (1659.68 cm^{-1}), amide II (1543.58 cm^{-1}), amide III (1241.34 cm^{-1}); deformation peaks (562.8 and 603.78 cm^{-1}) and stretching (1031.46 cm^{-1}) vibrations of calcium orthophosphates, absorption bands of the anion CO_3^{2-} (871.93 , 1417.66 and 1451.44 cm^{-1}) and those of methyl CH_2 and CH_3 groups (2925.06 cm^{-1}).

In the IR absorption spectra of the studied samples from the mandible and horn of the woolly rhinoceros (F-507 and F-509), the peaks of the same components were detected and interpreted (Fig. 6, Tables S2, S3).

The IR absorption spectra of the bone tissue of the mandible (Fig. 6A–C) and horn (Fig. 6D) of the woolly rhinoceros are similar to those in other well-preserved mammal specimens, especially in the region of absorption bands of the organic component.

Discussion

Factors that cause blackening of bones

The carbonization or charring of fossil bones, associated with wildfires or human activities, is accompanied by the destruction primarily of collagen. In such cases, the blackening of organic matter is usually associated with fire action and is the product of incomplete combustion of plants, bone, soft tissues, etc. However, bones that have undergone various types of nonpyrogenic factors also acquire blackening externally, which resembles charring.

Mineralization. – Blackening by mineralization is acquired by the remains of mammals in alluvial sediments

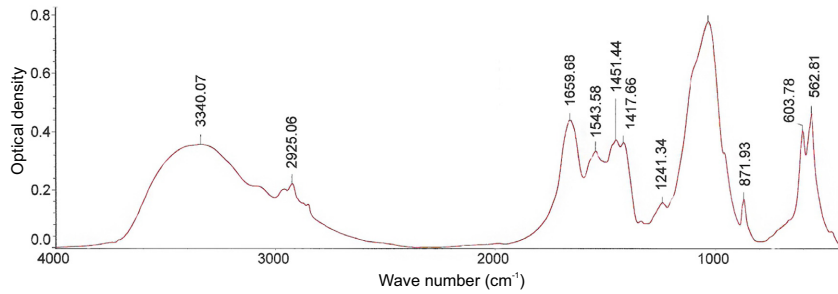


Fig. 5. IR spectra of the control sample.

lying on water-impermeable beds, with running water saturated with salts of iron and manganese. In the Lower Volga River basin on water-impervious clays at the base of Chernoyarsk alluvium in the bone bed many mammal fossils have a dark brown to black colour resulting from the water containing dissolved metal salts (Fig. S3); smaller bones are coloured completely through.

Nonpyrogenic black staining of mammal fossils is widely known (e.g. Retallack *et al.* 2018). A prominent example would be the very mineralized bones of different ages from the Netherlands that once were known as the ‘black bone fauna’ of the Pretiglian age (Hooijer 1981). The bones are black and black-brown in colour and have high specific gravity. These bones and others from different regions show that the colour of bone is strongly influenced by environmental factors, which can vary significantly in space and time (Drees 1986).

Humid anaerobic conditions. – Osseous remains of modern mammals acquire a black colour when exposed to microorganisms and metal salts under humid conditions, including in sediments of high latitudes. A forensic study of near-surface burial in sands less than 100 years old on the Island Bely in the Kara Sea revealed a significant blackening of bones (Fig. S4). According to the archival data, there had been no impact of thermal factors at this burial site (Pletyanova 2016). Burial in the seasonally active layer access for moisture and microorganisms which led to the superficial blackening of the human remains. The main factor of the colour changes, probably, was the gel-type hydrotroilite ($\text{FeS}_n \cdot \text{H}_2\text{O}$) mineral, which formed under anoxic conditions due to microbial activity (Gavrilov 2010).

Indirect charring. – Indirect charring sometimes is expressed in blackening of the innermost part of a bone only, while its surface preserves lighter colours depending on the host soil/rock composition. For instance, horse bones from the burial mound Tc-255 in the medieval archaeological complex Gnezdovo (Smolensk region, central European Russia) were blackened inside but not on the outer surface. During the excavation of the mound, signs of charring on the surface of the bones were not visible, which was why the burial had been

erroneously classified as inhumation. After destruction of the outer greyish-yellow compact bone in some places, a strongly charred spongy tissue was exposed. This relatively low-temperature charring could have developed indirectly as a result of a nearby fire because the burial pit was bordered by a dark ash ring and underlain by sand impregnated with ash and charcoal fragments (Kirillova & Spasskaya 2015). As a result, the uneven thermal transformation of the symmetrical bones of the right and left sides of the horse skeleton is observed because these bones were different distances from the heat source (Fig. 7).

Activity of thermophilic bacteria. – Thermophilic bacteria and biochemical processes are other factors that drastically change conditions under which the burial processes take place. For instance, in veterinary practice, so-called biothermal pits are used for the disposal of carcasses of domestic farm animals where the temperature inside the heap of densely packed corpses rises to 57–65 °C for 15 days and remains at this level for several days more (Miller & Flory 2018). The decomposition of carcasses in the pit ends in 40 days with the formation of homogeneous compost. Cattle dung decomposes in the same way (Lvov 1953). Such processes do not necessarily lead to charring of animal remains but can facilitate spontaneous combustion, in which the temperature reaches 200–300 °C and higher. As a result, pyrogenic charring can occur.

Similarly, significant accumulations of plant litter typical of eastern Siberian *alas* thermokarst depressions, which existed from at least the Late Pleistocene, often lead to spontaneous developments of natural ‘biothermal pits’ where high temperature results from microbial processes and facilitates self-ignition of the plant litter with a subsequent emergence of wildfires (Taubkin 2016).

Such processes could ultimately lead to complete carbonization of bones accumulated in *alas* depressions.

Possible factors contributing to the blackening of the studied fossils

The IR study revealed that the mineral component of the samples was somewhat changed, especially with regard

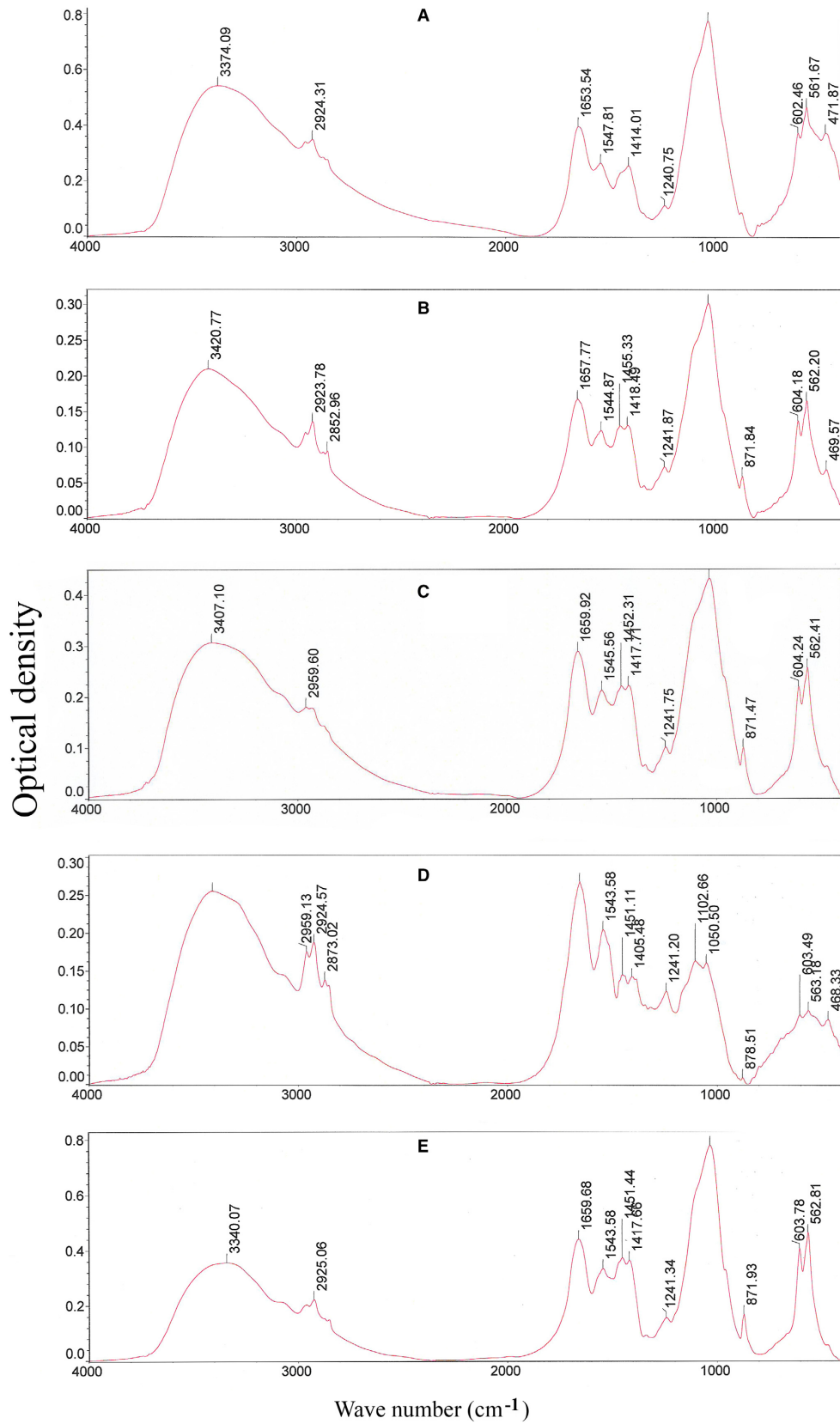


Fig. 6. IR absorption spectra of the woolly rhinoceros derivatives. A, B, C. Samples 1, 2 and 4 (mandible F-509), respectively. D. Sample 3 (nasal horn F-507). E. Control sample from Fig. 5 for comparison.

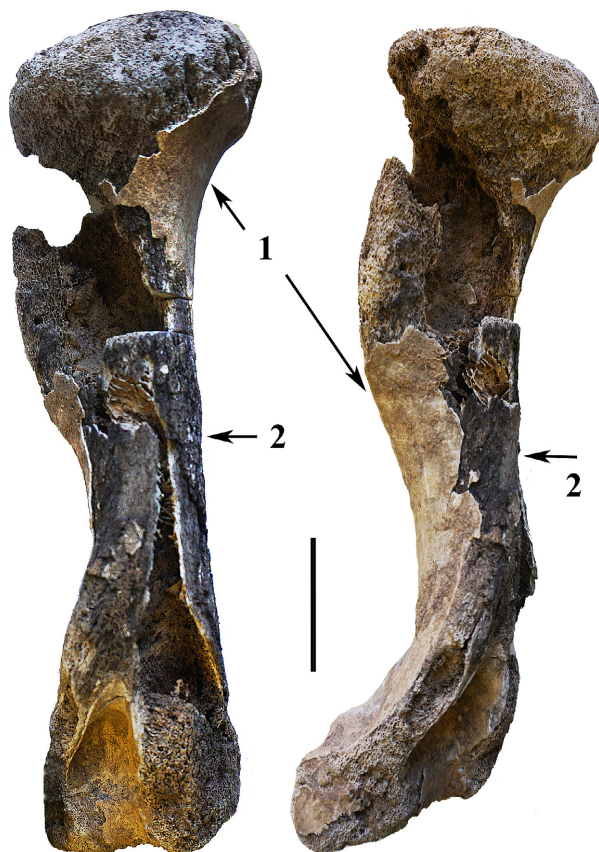


Fig. 7. Humerus of a horse from the burial Ts-255 Gnezdovo, collection S-186120. 1 = Outer layer of the compact bone without charring, rear view; 2 = charred spongy bone in areas where the compact tissue was crumbled during burial, side view. Zoological Museum, Lomonosov Moscow State University. Scale bar: 5 cm.

to the horn, where splitting and a significant decrease in the intense absorption bands associated with orthophosphate regions at $400\text{--}650$ and $900\text{--}1150\text{ cm}^{-1}$ were detected as well as those associated with carbonate. Similar changes are observed in bone tissue from the mandible (F-509) where alternations are especially pronounced in its presumably charred part. The IR spectrum of the less altered part of the mandible (F-509) is quite consistent with the normal spectrum of the native bone. As organic components of bone tissue are preserved, changes in the orthophosphate region can be produced by external factors influencing its mineral components only such as an acidic environment.

A temperature range of $400\text{--}500\text{ }^{\circ}\text{C}$ primarily will affect the peaks of amides (starting from III), leaving the mineral component intact. To obtain this effect, the protein and residual water have to be removed from bone during high temperature ashing. The optimal mode of ashing of bone and cartilage is subjecting a specimen to temperatures of $400\text{--}500\text{ }^{\circ}\text{C}$ for 1.5 h. The IR spectra of enamel, dentin, and cementum after such a treatment would be characterized by well-expressed absorption

bands of the inorganic part, with the simultaneous disappearance of bands of the organic part and water residues (Mikhailov *et al.* 1987).

In the studied samples the IR pattern is the opposite, and we can confidently assert the absence of thermal effects on the charred nasal horn F-507 and the mandible F-509, as well as on the skull and frontal horn from the same individual. The IR spectra of bone and horn are identical (Fig. 6A–C). They are characterized by the presence of peaks of all three amides of sufficient intensity, the absence of lipids, and a noticeable destruction of the spectrum at regions of inorganic components (especially orthophosphates) expressed in splitting of peaks and a decrease in intensity, which is most pronounced in sample 3 (F-507). Forensic studies have observed similar changes with prolonged exposure of bones to acidic factors, i.e. under conditions of ‘wet (acidic) ashing’ (Zvyagin 2009). Wet (acidic) ashing of organic matter was produced artificially *in vitro* at temperatures above $120\text{ }^{\circ}\text{C}$ in the presence of a large amount of an oxidizer such as acid solutions of high concentration (Bobritskaya 1958).

The absence of wildfires as a factor that caused charring was confirmed by the study of two fragments of the F-1990 specimen (from the surface and from the inside) on a Paragon 500 Perkin Elmer IR-spectrophotometer. There was significant destruction of orthophosphate while the organic matter was well preserved (Kirillova *et al.* 2019). Neither of the other aforementioned factors of blackening was involved in the colour alteration of specimens studied here because each of them would have been expressed either as an even tinting of the bone material or as complete charring of bones with destruction of biomineral components.

Processes that produce features resembling charring occur in the soil during the decomposition of plant litter. The possibility of black carbon forming in the organic matter by nonpyrogenic pathways has been experimentally proven to occur in soil under aerobic conditions (Chen *et al.* 2020). Similar features are observed as a result of oxidation of organic matter during prolonged intervals of degradation (Semenov *et al.* 2013). Nonpyrogenic charring occurs in soil or peat in the presence of excess water and catalysts in the form of Fe^{+2} , Mg^{+2} and some other cations. Surface oxidation of organic particles occurs in the presence of free oxygen. Under arid conditions, oxidation is due to the photochemical energy of the sun. In all cases, the process can last hundreds of years. Organic matter at the same time acquires a surficial blackening and does not completely decompose but stabilizes to persist for a long time.

The reserves of organic carbon (C_{org}) in the metre-thick upper layer of modern sediments/soils of the Kolyma lowland average about 18%. In these organic-rich strata, C_{org} is about 25–30%, while in the siliclastic layers it is 1–2% (Khodzhaeva *et al.* 2020). The organic-rich layers of buried soils contain up to 5%

of C_{org} , in the yedoma 0.6–2.8% (Zanina et al. 2011). During episodes and epochs of warming, the processes of organic matter accumulation and its degradation were intensified.

Genesis of infilling sediment from studied specimens and palaeoenvironment of their burial

In terms of the ratio of clay/silt/sand fractions, the infilling sediment of skulls F-506 and F-61 is similar to modern yedoma covering vast areas in northeastern Russia, but there are also differences: the yedoma of the Indigirka River basin is characterized by bi- and poly-modal particle-size distribution with a primary mode of ~41 μm (coarse silt) and subsidiary modes of very fine clay to fine sand size range (Murton et al. 2015). Alluvial sediments may be regarded as the alternative source of the studied material. However, despite the discovery of the F-506 skull at the river bottom, the fine composition and good sorting of sediments are inconsistent with the alluvial facies which are expected to have more sandy composition in the rivers of this region. The much finer composition of sediments filling the skull is typical for the overbank deposits. The insignificant content of sand indicates that the sediments accumulated at a fairly long distance from the main channel – in the central or rear part of the wide river flood-plain. The skull F-506 probably was buried in a river flood-plain, which became an alluvial terrace that was later eroded by river migration. The organic matter content of slightly over 6%, determined by the loss of mass during calcination at 550 °C, is quite typical both for yedoma silts (Murton et al. 2015) and flood-plain sediments. Thus, according to the grain-size range, the infilling sediments of the skulls F-506 and F-4299 (Fig. 4) could have originated from either the yedoma or flood-plain deposits, and judging by presence of the sponge spicules and abundant intact extremely delicate diatomean frustules the latter is more likely. All found diatoms are benthic and include freshwater species, which inhabit mainly cold oligotrophic waters including rivers, lakes, and swamps. Spicules are derived from either *Spongilla* or *Ephydatia* sponge species, which inhabit standing and running fresh and brackish waters including the permafrost zone in the Northern Polar Cycle (Manconi & Pronzato 2002). The fragmented nature of these megascleres as well as the absence of microscleres and gemmuloscleres suggest a long-term transportation of spicules to the burial place of the rhinoceros skull.

In turn, the presence of rare pollen of aquatic plants (*Myriophyllum*, *Potamogeton*), leaf spines of *Ceratophyllum* and coenobia of *Botryococcus* and *Pediastrum* in the specimen F-506 as well as rare pollen of typical coastal plants (*Typha latifolia* and *Sparganium*) and the abundance of *Riccia* spores also indicate the probable fluvial genesis of the infilling sediments. Ecological studies of Siberian species of genus *Riccia* have revealed that the

main habitats of *Riccia* species are muddy shallow river banks (Bakalin & Taran 2004). The composition of NAP reflects the presence of rich meadow vegetation. Over 15 families of forbs are represented in this specimen, many of them by several morphological types of pollen. Such a diversity even in the southern tundra zone is achieved only in the flood-plain meadows where soil properties, moisture conditions and microclimate are milder than on the interfluves.

The composition of AP in specimen F-506 shows that the climatic conditions at the time of burial of the woolly rhinoceros remains were somewhat warmer than modern, since at present neither tree birch (*Betula pendula*) nor shrub birch (*B. fruticosa*) reaches the basin of the Malaya Kuropatochya River (Lomonosova et al. 1992). Shrub alder occurs only at its upper reaches, while in the F-506 specimen pollen of *Alnaster fruticosus* makes up almost 7% of Σ . The specimen contains pollen from pines of both subgenera and even spruce (apparently wind-blown), which is absent in the modern and Holocene spectra in this region. Among other palynomorphs in the same specimen, a variety of fungal spores were found, including *Glomus*, which supposedly indicates soil erosion, and *Gelasiospora*, a fungus that develops on herbivore dung. The presence of spores of coprophilous fungi and pollen of meadow plants suggests the existence of rich pastures that developed in flood-plain meadows and in the overgrown alas thermokarst depressions.

Dominance of large-sized (50–100 μm) phytoliths indicates a rather tall vegetation. Trichomes with a wide base are found in many species of grasses and are formed in outgrowths of the epidermis (e.g. hairs, tubercles, spines). Among the Poaceae family, trichomes are developed in long-rooted grasses that grow in areas with sufficient and excess moisture (Speranskaya et al. 2016). Large-sized (up to 70 μm) phytoliths are found in the Lower Kolyma River basin in modern grasses *Calamagrostis purpurea*, *Arctophila fulva* and *Agrostis* sp., which often reach 1.5 m in height and form thickets along the banks of rivers, lakes and streams as well as on flooded meadows and river ramparts (Berkutenko et al. 2010).

The abundance of aquatic plant remains most likely indicates the genesis of the infilling sediments in a damp meadow with dense and high motley herbs and grasses.

Palynological data on sample F-61 from the Lower Indigirka River make it possible to reconstruct the surrounding vegetation as open larch-subshrub-lichen-moss forests (northern taiga), possibly with some tree birch participation, with patches of sedge/grass bogs in the depressions. The rhinoceros corpse was probably buried in the palustrine soil in such a bog depression with dense grass-sedge vegetation, at the edge of a larch stand with an undergrowth of willow, shrub birches, and alder, with *Sphagnum* and the Ericales dwarf shrubs in the ground cover. Besides, the specimen contains microscopic fragments of sedge roots, bark and wood of birch

and alder, fragments of coniferous tracheids, as well as spores of *Chaetomium* and *Dictyosporium*, fungi that develop on decaying organic matter and dead wood. Numerous spores and hyphae of *Glomus* fungi that form mycorrhiza on plant roots were also found. Findings of pollen of plants typical of disturbed soils and of pioneer taxa such as *Rumex*, *Plantago*, *Urtica*, Onagraceae and Asteraceae also indicate the influence of solifluction and/or water erosion.

In general, the composition of the pollen and other microfossils allows us to conclude that during the burial of the woolly rhinoceros F-61, the climatic conditions in the region were close to modern ones and possibly somewhat milder. Pollen from such anemophilous trees as *Betula pendula*, *Picea obovata* and *Pinus sylvestris* occurred in the studied specimen as a result of long-distance wind transportation.

Taphonomic keys to the burial conditions

The Late Pleistocene yedoma deposits, widespread in northeastern Russia, are subdivided into four climatostratigraphical horizons: Kazantsevo – MIS 5, Zyryanka (Yermakovka) – MIS 4, Karga – MIS 3, and Sartan (latest Zyryanka) – MIS 2. The MIS 5 and 3 were relatively warm episodes, the MIS 4 and 2 were colder.

Palaeopedological study of the most complete sections of the Kolyma lowland (Duvanny Yar, Stanchikovskiy Yar, and Green Cape near the Chersky township) revealed four profiles of buried soils within MIS 3 strata, namely in ascending order the early Karga (>40 ka) and three late Karga intervals (I: 37–35 ka, II: 33–31 ka and III: c. 28 ka). The soils were formed during brief warmings leading to seasonally thawed grounds. The increase in temperature and humidity allowed the development of a variety of herbaceous and shrubby vegetation; wetlands overgrown with sedge were formed in waterlogged areas over sizable ice wedges. Peat accumulation occurred due to excess moisture in the topographic depressions (Zanina *et al.* 2011; Gubin & Zanina 2014). Thus, buried soils and autochthonous peatlands are markers of climate ameliorations recorded in sections.

We suggest that the charring of fossils due to wet ashing is an additional mark of the environment and time of accumulation of the infilling sediments. Obviously, certain conditions must be in place to preserve mammal remains. The most common traps for large mammals in the permafrost zone are gullies filled with thawed soil, muddy bottoms of freshwater basins, yedoma landslides, and ice cracks, among others, the formation of which was restricted to warm seasons. Thus, the composition of the trapping sediments is very important: in cases with the best preserved corpses of large Pleistocene mammals, their fine-grained composition and vivianite mineralization of soft tissues were noted (Guthrie 1990; Boeskorov *et al.* 2011; Fisher *et al.* 2014); the latter indicates anoxic conditions.

In addition to wet ashing, taphonomic changes of Late Pleistocene (MIS 3, MIS 5e) mammal bones, skins, and inner organs are commonly accompanied by vivianite formation (e.g. Guthrie 1990; Fisher *et al.* 2014; Kirillova *et al.* 2020). For instance, the presence of this iron phosphate [$\text{Fe}_3(\text{PO}_4)_2 \cdot 8\text{H}_2\text{O}$] is observed on Late Pleistocene mummies representing the mammoth fauna (Fig. 8, Table 2). A number of such remains are restricted to the Karga interstadial (MIS 3; 50–26 ka), namely, the Kirgilyakh mammoth calf (41 ka), Tirekhtyakh (44–36 ka) and Shadrin (42–36 ka) mammoths, the Selirikan horse (37 ka) and some others (Tomskaya 2000).

The precipitation of this authigenic hydrous phosphate mineral of ferrous iron requires a number of specific conditions, which are organic-rich and iron-rich, sulphate-poor acidic reductive fresh waters (less commonly this mineral is formed in waterlogged soils and coastal marine sediments); its nucleation in natural systems is maintained by the activity of metal reducing, mostly anaerobic, bacteria (Rothe *et al.* 2016). Fine-grained vivianite commonly forms in cold lacustrine settings (Manning *et al.* 1991). The source of the principal components of this mineral is mainly organic-bound phosphorus commonly associated with decaying organic remains (McGowan & Prangnell 2006) and dissolved ferric iron efficiently scavenging orthophosphate under anoxic conditions and being subsequently reduced to ferrous state (Cosmidis *et al.* 2014). Pristine vivianite is colourless but, upon exposure to air, a gradual oxidation of ferrous iron leads to its colour alteration, while the intensity of the blue colour depends on ferric ion concentrations (Manning *et al.* 1991).

In the case of the bison skull (F-4236) described here and many other Ice Age mammal remains, including a number of complete bodies (Table 2), abundant authigenic vivianite was probably formed by the substantial phosphate supply from the remains themselves. The sources of iron were the cold water bodies of eastern



Fig. 8. Anyuy ancient bison mummy intensely encrusted by vivianite, F-3210. National Alliance of Shidlovskiy 'Ice Age', Moscow.

Table 2. Ice Age mammal body remains coated with vivianite.

Specimen	Area	Age, geochronological (^{14}C a BP)/chronostratigraphical	Reference
Rauchua bison	NW Chukotka	c. 9500/Holocene	Kirillova et al. (2015)
Yukagir bison	N Yakutia	9600–10 500/Holocene	van Geel et al. (2014)
Kastykhtakh mammoth	W Taimyr	32 070–30 565/MIS 3	Kirillova et al. (2012)
Blue Babe bison	Alaska	36 000/MIS 3	Guthrie (1990)
Bilibino horse	NW Chukotka	37 000–31 000/MIS 3	Spasskaya et al. (2012)
Kolyma rhinoceros	NE Yakutia	39 000/MIS 3	Boeskorov et al. (2011)
Mammoth calf 'Lyuba'	Yamal Peninsula	41 800/MIS 3	Fisher et al. (2014)
Mammoth calf 'Zhenya'	W Taimyr	c. 48 000/MIS 3	Mashchenko et al. (2017)
Anyuy bison	NW Chukotka	50 000–35 000/MIS 3	Nikolskiy & Shidlovsky (2014)
Khroma mammoth calf	NE Yakutia	Over 50 000	Mashchenko et al. (2013)

Siberian bogs and thermokarst lakes, which are enriched in this element (Kumke et al. 2007).

Bison skull F-4236 (Fig. 3B) is characterized by charring of the horn covers, which hints at aerobic conditions, and vivianite encrustation of the skull itself, which is typical of an anaerobic milieu. The development of these seemingly mutually exclusive features has two possible explanations. Either these traits were acquired sequentially, with surface charring first and then immersion in the swampy ground under anoxic conditions, or, less likely, the skull was only partially immersed in swamp sediments at the border of two different redox environments. The subsequent complete covering with sediments preserved the skull with these features. As well, the bison skull could have been reburied quickly from one condition to another.

In general, accelerating anaerobic bacterial activity during warm seasons was among the principal factors responsible for the vivianite precipitation on the bones and bodies. Dentin and tooth enamel coloured with vivianite crusts as well as with other iron salts indicate a sufficiently long stay of mammal remains in a humid chemically active environment, such as shallow lake water or a river oxbow with a temperature allowing the dissolving of active phosphorus in liquid and its following deposition. Such processes were activated during the degradation of permafrost and the formation of lake-alluvial landscapes in the warm phases of the MIS 3 interstadial and interglacial (for example, in MIS 5e; Kirillova et al. 2020). Accumulations of animal organic matter rich in phosphorus could have occurred due to the death of large herbivores as a result of falling into natural traps developed during episodes of warming.

The composition of pollen and spores found in specimen F-506 (Table S1) is indicative of the development of southern (shrub) tundra and birch forest-tundra with a small participation of larch in the Malaya Kuropatochya River basin during a warming when the burial of the rhinoceros remains occurred. The pollen composition reflects the presence of rich meadow vegetation and widespread grass and moss bogs. The specimen contains pollen of *Rubus chamaemorus*, which grows in moist moss and moss-lichen tundra and on

Sphagnum bogs. At present, the northern border of this vegetation type is approximately at the headwaters of the Malaya Kuropatochya River. Of the subaquatic plants indicated in the specimen, nowadays *Sparganium* species only reach the Lower Kolyma River basin in the north while the nearest modern habitats of *Typha latifolia* are located in the Lena River basin, south of 65°N (Kashina et al. 1988). Of the aquatic plants, neither *Potamogeton* nor *Myriophyllum* occurs at present in the Malaya Kuropatochya River basin (Kashina et al. 1988).

Equally significant, the composition of pollen, spores, and other palynomorphs from specimen F-61 is indicative of rather mild climatic conditions in the Lower Indigirka River basin during the burial of another woolly rhinoceros, conditions that were close to modern ones and possibly even warmer.

Thus, with the development of birch forest tundra, the pollen spectrum of which is identified in the specimen F-506 (Table S1), the most important implication is not so much the degradation of the permafrost, but summer thawing that was deeper than in the modern tundra. Evidence of such thawing is the presence in yedoma silts of thick lacustrine sediment bodies and refrozen Taber ice deposits (with a characteristic loss of original cryostructures), palustrine deposits with peat blocks, grass roots, lenses of organic matter, moss, and sedge bumps. The latter are found in the 'warm' yedoma MIS 3 strata more often than in the glacial MIS 2 ones. Their emergence and development are associated with changes in climatic regimes from harsh continental to milder, with an increase in temperature and humidity (Kaplina 2011). During the warming episodes MIS 5e and MIS 3, natural traps and conditions facilitating burial of mammal remains were widely developed.

Conclusions

The present study revealed that the charring of specially selected Late Pleistocene mammal skulls from the permafrost zone of northeastern Russia was nonpyrogenic and occurred under the influence of biochemical processes during the decomposition of organic matter due to wet (acidic) ashing. This conclusion is upheld with

data from the IR spectrophotometry for the woolly rhinoceros nasal horn (F-1990), the cave lion skull (F-4299) and also probably for bison and woolly rhinoceros skulls (F-4236 and F-61) of the studied sampling set. IR spectra indicate relatively good preservation of the bone organic content whereas its mineral compounds are altered due to charring.

We assume that the charring was a result of wet ashing (under oxic conditions) while the vivianite encrustation (occurring under anoxic conditions) indicates mammalian remains were buried during relatively warm epochs. These data can serve as a reliable diagnostic feature of age and stratigraphical position of mammal fossils collected outside outcrops.

Based on the ^{14}C dating, three samples with traces of charring are associated with long-term complex interstadial warming corresponding to MIS 3. The burial times of the bison (F-4236) and woolly rhinoceros (F-506–F-509) correspond to the earliest warm episode of the Karga interstadial while the cave lion (F-4299) was trapped during the latest one. Palynological and other microfossil data of the sediments infilling brain cases of the skulls F-506 and F-61 confirm the results of ^{14}C dating restricting their burial time to episodes of warming similar to present day conditions or even to milder climates.

Acknowledgements. – The authors are grateful to F.K. Shidlovskiy for materials from northeastern Russia and the Zoological Museum of the Lomonosov Moscow State University for access to the horse bones from the burial of Tc-255 Gnezdovo, to G. Ehrlich for a discussion of the IR spectra, to Z.V. Pushina for identification and discussion of diatoms, A.A. Gol'eva for help with the palaeobotanical data, V.M. Semenov and V.O. Lopez de Guerinu for consultations on the soil organic matter alterations, M.A. Bronnikova, P.I. Kalinin and G.V. Mitenko are thanked for advice on the geochemistry of the permafrost. The study was partially supported by M.P. Kirillova. Phytolith analysis was carried out within the State Theme IPCBPSS RAS and within the RFBR Project No. 20-05-00559 A (O.G. Zanina). Palynological and lithological studies contribute to the IGRAS State Theme 0148-2019-0005 (O.K. Borisova, A.V. Panin). We are deeply indebted to Prof. Jelle W.F. Reumer and the anonymous reviewer for their valuable comments and recommendations.

Author contributions. – IK, OC, AZ and GH – description, discussion and editing; OB and OZ – palaeobotany; EZ – radiocarbon dating; AP – grain-size analysis; NN and VZ – IR spectrophotometry.

References

- Bakalin, V. A. & Taran, G. S. 2004: The genus *Riccia* L. (Hepaticae) in Siberia and the East Kazakhstan. *Botanical Journal* 89, 1283–1294.
- Berkutenko, A. N., Lysenko, D. S., Khoreva, M. G., Mochalova, O. A., Polezhaev, A. N., Andriyanova, E. A., Sinel'nikova, N. V. & Yakubov, V. V. 2010: *Flora and Vegetation of the Magadan Region (Checklist of Vascular Plants and Outline of Vegetation)*. 364 pp. Institute of Biological Problems of the North, Far East Branch, Russian Academy of Sciences, Magadan (in Russian).
- Bobritskaya, M. A. 1958: *Methods of the Ash Analysis of Plants*. 39 pp. V.V. Dokuchaev Soil Institute, Moscow (in Russian).
- Boeskorov, G. G., Lazarev, P. A., Sher, A. V., Davydov, S. P., Bakulina, N. T., Shchelchikova, M. V., Binladen, J., Willerslev, E., Buigues, B. & Tikhonov, A. N. 2011: Woolly rhino discovery in the lower Kolyma River. *Quaternary Science Reviews* 30, 2262–2272.
- Bronk Ramsey, C., Higham, T., Bowles, A. & Hedges, R. 2004: Improvement to the pretreatment of bone at Oxford. *Radiocarbon* 46, 155–163.
- Brown, T. A., Nelson, D. E., Vogel, J. S. & Southon, J. R. 1988: Improved collagen extraction by modified Longin method. *Radiocarbon* 30, 171–177.
- Chen, X., Ye, X., Chu, W., Olk, D. C., Cao, X., Schmidt-Rohr, K., Zhang, L., Thompson, M. L., Mao, J. & Gao, H. 2020: Formation of char-like, fused-ring aromatic structures from a nonpyrogenic pathway during decomposition of wheat straw. *Journal of Agricultural and Food Chemistry* 68, 2607–2614.
- Chernova, O. F. & Kirillova, I. V. 2010: New data on the morphology of the woolly rhino horn (*Coelodonta antiquitatis* Blumenbach, 1799). *Proceedings of the Zoological Institute of the Russian Academy of Sciences* 314, 333–342 (in Russian).
- Cosmidis, J., Benzerara, K., Morin, G., Busigny, V., Lebeau, O., Jézéquel, D., Noël, V., Dublet, G. & Othmane, G. 2014: Biomineralization of iron-phosphates in the water column of Lake Pavin (Massif Central, France). *Geochimica et Cosmochimica Acta* 126, 78–96.
- Drees, M. 1986: Kritische kanttekeningen bij de naam 'Zwarte botten fauna'. *Cranium* 3, 103–120.
- Fisher, D. C., Shirley, E. A., Whalen, C. D., Calamari, Z. T., Rountrey, A. N., Tikhonov, A. N., Buigues, B., Lacombe, F., Grigoriev, S. & Lazarev, P. A. 2014: X-ray tomography of two mammoth calf mummies. *Journal of Paleontology* 88, 664–675.
- Gavrilov, Y. O. 2010: Diagenetic migration of sulfides in sediments accumulated in different sedimentation settings. *Lithology and Mineral Resources* 45, 120–135.
- van Geel, B., Fisher, D. C., Rountrey, A. N., van Arkel, J., Duivenvoorden, J. F., Nieman, A. M., van Reenen, G. B. A., Tikhonov, A. N., Buigues, B., & Gravendeel, B. 2011: Palaeoenvironmental and dietary analysis of intestinal contents of a mammoth calf (Yamal Peninsula, northwest Siberia). *Quaternary Science Reviews* 30, 3935–3946.
- van Geel, B., Protopopov, A., Bull, I., Duijm, E., Gill, F., Lammers, Y., Nieman, A., Rudaya, N., Trofimova, S., Tikhonov, A. N., Vos, R., Zhilich, S. & Gravendeel, B. 2014: Multiproxy diet analysis of the last meal of an early Holocene Yakutian bison. *Journal of Quaternary Science* 29, 261–268.
- Giles, M. 2020: *Bog Bodies. Face to Face with the Past*. 312 pp. Manchester University Press, Manchester.
- Grichuk, V. P. 1940: Technique of processing of sedimentary rocks, poor in organic matter, for pollen analysis purposes. *Problems of Physical Geography* 8, 53–58 (in Russian).
- Gromov, V. I. 1948: Palaeontological and archaeological grounds for the stratigraphy of terrestrial strata of the Quaternary Period on the USSR territory (mammals, Palaeolithic). *Transactions of the Institute of Geological Sciences, Academy of Sciences of the USSR* 64, *Geological Series* 17, 1–522 (in Russian).
- Gubin, S. V. & Zanina, O. G. 2014: Variations of soil cover during the ice complex deposit formation, Kolyma Lowland (Part 2). *Earth's Cryosphere* 18, 77–82 (in Russian).
- Guthrie, R. D. 1990: *Frozen Fauna of the Mammoth Steppe: The Story of Blue Babe*. 323 pp. University of Chicago Press, Chicago.
- Haynes, G. 1981: *Bone modifications and skeletal disturbances by natural agencies: studies in North America*. Ph.D. thesis, Catholic University of America, 527 pp.
- Haynes, G. 1988: Mass deaths and serial predation: Comparative taphonomic studies of modern large mammal death sites. *Journal of Archaeological Science* 15, 219–235.
- Hooijer, D. A. 1981: The first rhinocerotoid of the Pretiglian "black bones" fauna from the Netherlands. *Netherlands Journal of Zoology* 31, 472–475.
- Kaplina, T. N. 2011: Ancient alas complexes of northern Yakutia (Part 2). *Earth's Cryosphere* 15, 20–30 (in Russian).
- Kashina, L. I., Krasnoborov, I. M., Shaulo, D. N., Timokhina, S. A., Khanminchun, V. M., Danilov, M. P. & Kosterin, O. E. 1988. *Flora of Siberia, Volume 1: Lycopodiaceae – Hydrocharitaceae*. 200 pp. Nauka Siberian Branch, Novosibirsk (in Russian).

- Khodzhaeva, A. K., Shatilovich, A. V., Gubin, S. V. & Lupachev, A. V. 2020: Quantification of mineralizable pool of organic matter in tundra cryosols of Kolyma Lowland. *Eurasian Soil Science* 53, 215–222.
- Kirillova, I. V. & Spasskaya, N. N. 2015: Horse remains from the Gnezdovo archaeological complex, Smolensk Region, Russia. *Russian Journal of Theriology* 14, 85–104.
- Kirillova, I. V., Borisova, O. K., Chernova, O. F., Van Kolschoten, T., van der Lubbe, J. H. J. L., Panin, A. V., Pečnerová, P., van der Plicht, J., Shidlovskiy, F. K., Titov, V. V. & Zanina, O. G. 2020: ‘Semi-dwarf’ woolly mammoths from the East Siberian Sea coast, continental Russia. *Boreas* 49, 269–285.
- Kirillova, I. V., Borisova, O. K., Zazovskaya, E. P., Zanina, O. G., Zvyagin, V. N., Panin, A. V. & Shidlovskiy, F. K. 2019: Taphonomic aspect of charring of mammalian remains. *Abstract Volume of the All-Russian Scientific Conference Dedicated to the 90th Anniversary of L. D. Sulerzhitsky, Moscow, April 24–26, 2019*, p. 43. Institute of Geography, Russian Academy of Sciences, Moscow (in Russian).
- Kirillova, I. V., Shidlovskiy, F. K. & Titov, V. V. 2012: Kastykhtakh mammoth from Taimyr (Russia). *Quaternary International* 276–277, 269–277.
- Kirillova, I. V., Zanina, O. G., Chernova, O. F., Lapteva, E. G., Trofimova, S. S., Lebedev, V. S., Tiunov, A. V., Soares, A. E. R., Shidlovskiy, F. K. & Shapiro, B. 2015: An ancient bison from the mouth of the Rauchua River (Chukotka, Russia). *Quaternary Research* 84, 232–245.
- Kumke, T., Ksenofontova, M., Pestryakova, L., Nazarova, L. & Hubberten, H.-W. 2007: Limnological characteristics of lakes in the lowlands of Central Yakutia, Russia. *Journal of Limnology* 66, 40–53.
- Lazarev, P. A. & Tomskaya, A. I. 1987: *Mammals and biostratigraphy of the Late Cenozoic of Northern Yakutia*. 170 pp. YaF SO AN SSSR, Yakutsk (in Russian).
- Lomonosova, M. N., Bol’shakov, N. M., Krasnoborov, I. M., Kashina, L. I., Tupitsyna, N. N., Gel’tman, D. V. & Shemberg, M. A. 1992: *Flora of Siberia, Volume 5: Salicaceae – Amaranthaceae*. 312 pp. Nauka Siberian Branch, Novosibirsk (in Russian).
- Lvov, N. S. 1953: *Biothermal Decontamination of Dung*. 88 pp. Sel’khozgiz, Moscow (in Russian).
- Manconi, R. & Pronzato, R. 2002: Suborder Spongillina subord. nov.: freshwater sponges. In Hooper, J. N. A. & Van Soest, R. W. M. (eds.): *Systema Porifera. A Guide to the Classification of Sponges* 1, 921–1019. Kluwer Academic/Plenum Publishers, New York.
- Manning, P. G., Murphy, T. P. & Prepas, E. E. 1991: Pyrite and vivianite intervals in the bottom sediments of mesotrophic Narrow Lake, Alberta, Canada. *The Canadian Mineralogist* 29, 77–85.
- Mashchenko, E. N., Potapova, O. R., Vershinina, A., Shapiro, B., Streletskaya, I. D., Vasiliev, A. A., Oblogov, G. E., Kharlamova, A. S., Potapov, E., van der Plicht, J., Tikhonov, A. N., Serdyuk, N. V. & Tarasenko, K. K. 2017: The Zhenya mammoth (*Mammuthus primigenius* (Blum.)): taphonomy, geology, age, morphology and ancient DNA of a 48,000 year old frozen mummy from western Taimyr, Russia. *Quaternary International* 445, 104–134.
- Mashchenko, E. N., Protopopov, A. V., Plotnikov, V. V. & Pavlov, I. S. 2013: Specific characters of the mammoth calf (*Mammuthus primigenius*) from the Khroma River (Yakutia). *Biology Bulletin* 40, 626–641 (in Russian).
- McGowan, G. & Prangnell, J. 2006: The significance of vivianite in archaeological settings. *Geoarchaeology* 21, 93–111.
- Mikhailov, V. S., Sapozhnikov, M. A. & Shafranskiy, L. L. 1987: *Forensic Value of the Study of Human Teeth by Infrared Spectrophotometry (Manual)*. 78 pp. State Medical Institute, Alma-Ata (in Russian).
- Miller, L. & Flory, G. 2018: Carcass management for small- and medium-scale livestock farms - Practical considerations. *FOCUS ON* 2018, 1–8.
- Murton, J. B., Goslar, T., Edwards, M. E., Bateman, M. D., Danilov, P. P., Savvinov, G. N., Gubin, S. V., Ghaleb, B., Haile, J., Kanevskiy, M., Lozhkin, A. V., Lupachev, A. V., Murton, D. K., Shur, Y., Tikhonov, A., Vasil’chuk, A. C., Vasil’chuk, Y. K. & Wolfe, S. A. 2015: Palaeoenvironmental interpretation of yedoma silt (ice complex) deposition as cold-climate loess, Duvanny Yar, Northeast Siberia. *Permafrost and Periglacial Processes* 26, 208–288.
- Nemec, M., Wacker, L., Hajdas, I. & Gaggeler, H. 2010: Alternative methods for cellulose preparation for AMS measurement. *Radiocarbon* 55, 1358–1370.
- Nikolskiy, P. & Shidlovskiy, F. 2014: Preliminary data from the study of the intact 50 000 YBP frozen mummy of the Anyuy steppe bison (Anyuy River, Arctic Far East). In Kostopoulos, D. S., Vlachos, E. & Tsoukala, E. (eds.): *Abstract Book of the VIth International Conference on Mammoths and their Relatives, S.A.S.G., Special Volume 2*, p. 141. School of Geology, Aristotle University of Thessaloniki, Thessaloniki.
- Ozer, M., Mehmet, O. & Nihat, S. I. 2010: Effect of particle optical properties on size distribution of soils obtained by laser diffraction environment. *Engineering Geoscience* 16, 163–173.
- Pletyanova, I. V. 2016: The peculiarities of preservation of the soft tissues and bone structures under the conditions of prolonged corpse deposition in the high-latitude cryolitic zone (the Island Bely near the Kara Sea coast). *Forensic Medical Expertise* 59, 31–35 (in Russian).
- Puzachenko, A. Y., Levchenko, V. A., Bertuch, F., Zazovskaya, E. P. & Kirillova, I. V. 2021: Late Pleistocene chronology and environment of woolly rhinoceros (*Coelodonta antiquitatis* (Blumenbach, 1799)) in Beringia. *Quaternary Science Reviews* 263, 106994, <https://doi.org/10.1016/j.quascirev.2021.106994>.
- Reimer, P. J., Bard, E., Bayliss, A., Beck, J. W., Blackwell, P. G., Ramsey, C. B., Buck, C. E., Cheng, H., Edwards, R. L., Friedrich, M., Grootes, P. M., Guilderson, T. P., Hafflidason, H., Hajdas, I., Hatté, C., Heaton, T. J., Hoffmann, D. L., Hogg, A. G., Hughen, K. A., Kaiser, K. F., Kromer, B., Manning, S. W., Niu, M., Reimer, R. W., Richards, D. A., Scott, E. M., Southon, J. R., Staff, R. A., Turney, C. S. M. & van der Plicht, J. 2013: IntCal 13 and Marine13 radiocarbon age calibration curves 0–50,000 years cal BP. *Radiocarbon* 55, 1869–1887.
- Retallack, G. J., Martin, J. E., Broz, A. P., Breithaupt, B. H., Matthews, N. A. & Walton, D. P. 2018: Late Pleistocene mammoth trackway from Fossil Lake, Oregon. *Palaeogeography, Palaeoclimatology, Palaeoecology* 496, 192–204.
- Rothe, M., Kleeberg, A. & Hupfer, M. 2016: The occurrence, identification and environmental relevance of vivianite in water-logged soils and aquatic sediments. *Earth-Science Reviews* 158, 51–64.
- Scager, D. J., Ahrens, H.-J., Dieleman, F. E., van den Hoek Ostende, L. W., de Vos, J. & Reumer, J. W. F. 2017: The Kor & Bot collection revisited, with a biostratigraphic interpretation of the Early Pleistocene Oosterschelde Fauna (Oosterschelde Estuary, the Netherlands). *Deinsea* 17, 16–31.
- Semenov, V. M., Tulina, A. S., Semenova, N. A. & Ivannikova, L. A. 2013: Humification and nonhumification pathways of the organic matter stabilization in soil: a review. *Eurasian Soil Science* 46, 355–368.
- Sher, A. V. 1974: Pleistocene mammals and stratigraphy of the Far Northeast USSR and North America. *International Geology Review* 16, 1–284.
- Sher, A. V., Kuzmina, S. A., Kuznetsova, T. V. & Sulerzhitsky, L. D. 2005: New insights into the Weichselian environment and climate of the East Siberian Arctic, derived from fossil insects, plants, and mammals. *Quaternary Science Reviews* 24, 533–569.
- Smirnov, N. G., Votyakov, S. L., Sadykova, N. O., Kiseleva, D. V. & Shchapova, Y. V. 2009: *Physicochemical Characteristics of Mammal Fossil Bone Remains and the Problem of Their Relative Age Determination. Part 1: Thermal and Mass-Spectrometric Elemental Analysis*. 118 pp. Goshchitsky, Yekaterinburg (in Russian).
- Spasskaya, N. N., Kuznetsova, T. V. & Sher, A. V. 2012: Morphometric study of the skull of a Late Pleistocene mummy of the Bilibino horse from western Chukchi Peninsular. *Paleontological Journal* 46, 92–103 (in Russian).
- Speranskaya, N. Y., Solomonova, M. Y. & Kharitonova, E. Y. 2016: Phytoliths in some grasses of Altai region from different ecological groups and life forms. *Environmental Dynamics and Global Climate Change* 7, 155–162.
- Taubkin, I. S. 2016: Microbiological self-ignition as a cause of fire: guidelines for investigators and forensic examiners. *Theory and Practice of Forensic Science* 4, 73–85 (in Russian).

- Tomirdiaro, S. V. & Chernen'ky, B. I. 1987: Cryogenic Deposits of East Arctic and Sub Arctic. 196 pp. AN SSSR Far-East Science Center, Vladivostok (in Russian).
- Tomskaya, A. I. 2000: *Forage of the Late Pleistocene Mammoth in Yakutia*. 59 pp. Mammoth Museum, Institute of Applied Ecology of the North, Academy of Science of the Republic Sakha (Yakutia), Yakutsk (in Russian).
- Vereshchagin, N. K. 1979: *Why are Mammoths Extinct?* 195 pp. Nauka, Leningrad (in Russian).
- Zanina, O. G., Gubin, S. V., Kuzmina, S. A., Maximovich, S. V. & Lopatina, D. A. 2011: Late-Pleistocene (MIS 3–2) palaeoenvironments as recorded by sediments, palaeosols, and ground-squirrel nests at Duvanny Yar, Kolyma lowland, northeast Siberia. *Quaternary Science Reviews* 30, 2107–2123.
- Zvyagin, V. N. 2009: Yekaterinburg finds for 2007: The results of medical and forensic research. *Measurements World 2009*, 44–53 (in Russian).

Supporting Information

Additional Supporting Information to this article is available at <http://www.boreas.dk>.

Fig. S1. Diatoms from specimen F-506. 1 – *Ulnaria* sp. 2 – *Eunotia praerupta*. 3 – *Eunotia* sp. 1. 4 – *Eunotia* sp. 2. 5 – *Cocconeis placentula*. 6 – *Navicula radiosa*. 7 – *Navicula* cf. *cryptocephala*. 8 – *Stauroneis* sp. 9 – *Pinnularia eifelana*. 10 – *Pinnularia* sp. 11 – *Pinnularia borealis*. 12 – *Cymbella* sp. 13 – *Gomphonema* sp. 14 – *Didymosphenia geminata*. 15 – *Nitzschia* sp.

Fig. S2. Phytoliths from specimen F-506. 1–5 – Lobed trapezoid asymmetrical forms. 6 – Asymmetrical trapezoid. 7 – Globular particle. 8 – Trichomes with thorn. 9–11 – Trichomes with a wide base. 12 – Attenuate trichome. 13 – Elongate cylindrical smooth form. 14 – Elongate form with a wavy edge. 15 – Elongate parallelepipedal form. Scale bars, where not indicated: 20 μ m.

Fig. S3. Blackening of a rhinoceros talus due to iron and manganese salt tanning. A. Frontal view. B. Rear view. Scale bar: 5 cm.

Fig. S4. A recent human male skull blackened, probably, by microbial activity; exhumed and re-buried on the Island Bely, near the Kara Sea coast, under the regional project 'Kara Expeditions' patronaged by the government of the Yamal-Nenets Autonomous District, Russia, 2015 (photograph by I. V. Pletyanova).

Table S1. The results of pollen analyses of the sediments from the skulls of woolly rhinoceros F-506 and F-61.

Table S2. IR spectrophotometry data (optical density) of control samples (1 and 2) of bone tissue (region 4000.0–400.0, threshold 0.001, sensitivity 70).

Table S3. IR spectrophotometry data (optical density) of samples (1, 2, 4) of bone tissue of woolly rhinoceros (region 4000.0–400.0, threshold 0.001, sensitivity 70).